Find publisher's version under:
https://www.sciencedirect.com/science/article/pii/S0927024817306426

DETERMINATION OF CRITICAL THERMAL LOADS IN CERAMIC HIGH CONCENTRATION SOLAR RECEIVERS

Olena Smirnova, Thomas Fend[1], Raffaele Capuano, Gereon Feckler, Peter Schwarzbözl, Florian Sutter

German Aerospace Center, 51143 Köln, Germany

ABSTRACT

Solar towers with volumetric air receiver technology are a promising technology for continuous or demand oriented electricity supply from a sustainable resource with competitive costs. The absorber elements used for this receiver technology are permeable ceramic honeycombs, which are heated up by concentrated solar radiation. Afterwords the heat is being transferrd to air, which finally feeds the steam generator of a Rankine-Cycle. Resulting from the intensive solar flux of up to 800kW/m², the absorber modules are exposed to severe thermal loads. Maximum temperatures of more than 1000°C are reached. Furthermore, during daily start-up and shut down procedures and additionaly during cloud transitions the absorbers undergo transient heat loads, which might reduce their lifetime. The objective of the present study is to quantify the effect of typical thermal loads and to calculate the resulting mechanical stresses inside the absorber modules. Two types of absorbers have been compared, a conventional coarse honeycomb and an advanced one with a higher cellularity offering an improved efficieny potential. The mechanical strength of the cellular material is used to find out whether the computed thermomechanical stresses are critical or not. Finally, experimental thermo-shock tests have been carried out to validate the numerical models. It could be shown that under normal operation the thermomechanical stresses remain in a range markedly below the fracture stress in both absorber variants. As a

[1] Corresponding author

consequence, limits are given to what extent the material should be thermally loaded during operation.

1. INTRODUCTION

Some time ago, in the late 90ies of the last century, ceramics was assigned a promising future, because of its wide spectrum of use and its superior properties [1]. However, besides excellent strength and elasticity properties at high temperatures, ceramic materials show drawbacks concerning resistance to temporal and spatial thermal gradients. To overcome these problems a thorough prediction of the stresses due to thermal loads is necessary.

The study reported deals with the characterization of the thermomechanical properties of a siliconized silicon carbide (SiSiC) honeycomb structure, which is used as an open volumetric receiver for a solar tower. Thanks to its high application temperature of more than 1300°C SiSiC is the material of choice for high temperature applications in solar energy. However, since SiSiC – like monolithic ceramics in general – is not able to undergo plastic deformations, it is very sensible to thermo-shock loads. Thus, the main aim of the study is to find out determined limits for stationary and transient thermal loads during application in order to ensure a safe and durable operation of the system.

Numerous studies have been published since the mid 80ies of the last century dealing with SiSiC honeycomb structures applied as open volumetric receivers for concentrated solar radiation in solar tower technology. In this application, a large number of tracked mirrors direct the solar radiation to a central receiver on top a tower. This principle has been also realized and demonstrated in the experimental Solar Tower Jülich (Figure 1). The receiver of this plant consists of 1080 modular absorbers transferring the absorbed heat to an air flow, which finally feeds the boiler of a steam turbine. The absorber modules used are shown in Figure 2.

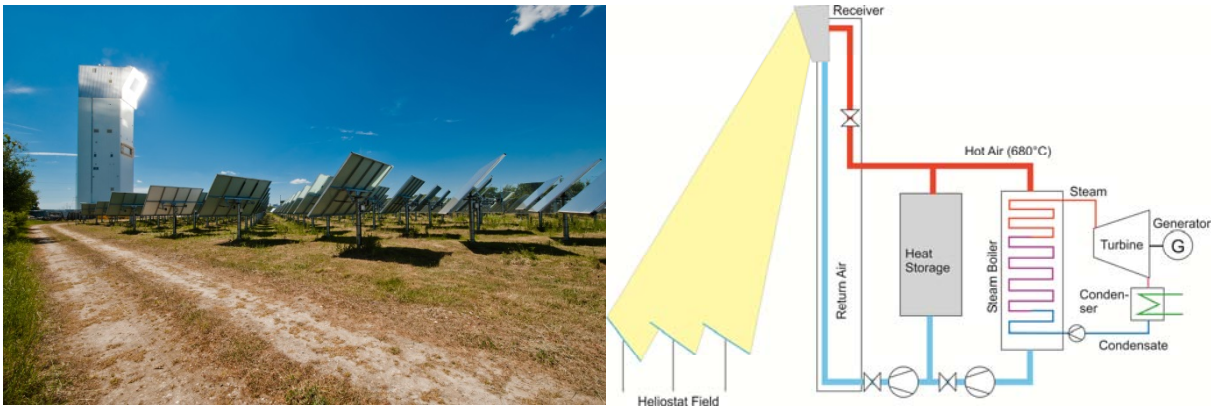

Figure 1. The Solar Tower Jülich and its working principle

Most of the studies focused on heat transport and solar-to-thermal efficiency [2-4]. A comparative review of these studies is presented in [5]. The honeycomb structure material's thermophysical and heat transfer properties are presented in [6]. A detailed analysis of the volumetric solar absorber along with experimental data of the thermomechanical properties before and after long-time thermal operation including pore size distribution, microstructure and influence of the manufacturing process is given by Agrafiotis [7]. Avilar-Marin and Hoffschmidt comprehensively describe the European projects HITREC II and SOLAIR under the leadership of the Spanish company Abengoa [8, 9]. They have been the basis for the development of the Solar Tower Jülich.

A review on the various technologies to model the fluid-dynamical and heat transfer phenomena of open volumetric receivers has been published by Capuano [10]. A thorough theoretical discussion of the constraints of the open volumetric receiver is given by Kribus [11]. He states that under certain conditions flow instabilities can occur, which may lead to an overheating of the receiver. Wu and co-workers [12] published an extensive study on heat transfer properties of ceramic foams foreseen as open volumetric receiver elements, which enabled them to subsequently present a detailed transient model to fully describe the performance of ceramic foam applied as an open volumetric receiver [13].

Common sense in these studies is the fact, that the general performance of a volumetric receiver is better if the material exhibits the following features: high cellularity (to create large surfaces for solid-to-gaseous heat transfer) and high porosity (to let the concentrated radiation deeply penetrate into the volume of the cellular structure). This has also been confirmed by a detailed parametric study based on a continuum model by Capuano [14]. Furthermore it has been shown that the effective thermal conductivity in the

direction perpendicular to the main flow direction directly influences the operation stability of the receiver. This can be achieved either by employing a material of high thermal conductivity (like the SiSiC in case of the HiTRec technology) or by a porous structure, which allows the fluid to move also in directions different from the main flow direction [15].

However, studies on thermal loads and their accompanying mechanical stresses have not yet been presented, although a precise knowledge on this topic could significantly improve the durability, safety and reliability of the receiver during everyday operation. On the one hand the overall operation experience of the solar volumetric absorber in solar tower technology has shown a good reliability of the structure, on the other hand the effect of critical temporal and spatial temperature gradients influencing the structure stability has not yet been investigated.

The current study aims at a thorough investigation of the influence of typical thermal loads occurring during regular operation on the mechanical stresses inside the absorber. Two types of structures have been considered: the standard one (80 cpsi[2])and an advanced one with a finer cell structure (200 cpsi, Figure 2).

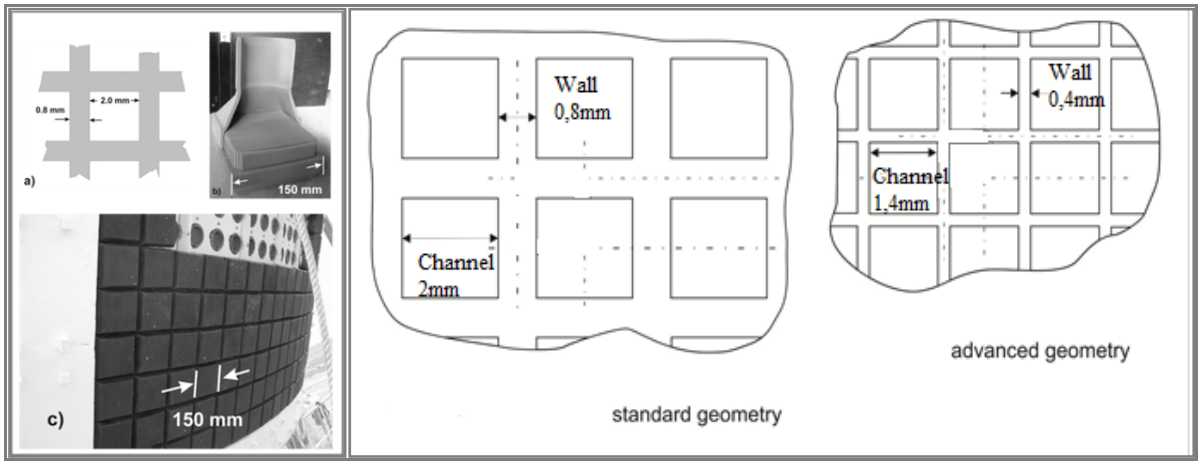

Figure 2**.** The modular receiver system of the Solar Tower Jülich (left), cross-sectional view of the absorber with cell density 80 cpsi (standard geometry) and 200 cpsi (advanced geometry)

[2] cpsi: cells per square inch

2. METHOD AND EXPERIMENTAL SET-UPS

2.1 General Procedure

The general procedure used to carry out the study has been as follows:

- Determination of a typical maximum thermal load during regular operation of an absorber in a Solar Tower
- Development of a coupled flow/heat transport model and calculation of the time-dependent temperature distribution, which corresponds to the thermal load defined in the first step
- Applying an appropriate thermomechanical model to compute the mechanical stresses, which arise as a consequence of the temperature distributions inside the component during operation
- Determination of the mechanical strength of the employed cellular material with conventional bending tests and comparison with computed thermomechanical stresses
- Performance of experimental thermo-shock tests and comparison of the results with data from the model calculation.

2.2 Determination of a typical maximum thermal load

As a maximum *thermal load* with a high temporal temperature gradient, which can possibly occur in everyday plant operation, a fast cloud transition has been considered. Since the heliostat field can have an approximate size of about 500 by 500 m it has been assumed, that a cloud takes 5 seconds to completely shift between the solar beam and the entire heliostat field. That means that the concentrated radiation density decreases from the lay-out operational value to zero in 5 seconds. Note that this shall cover an extreme case with high wind-speeds. After that, the cloud leaves the field with the same velocity.

From this consideration, a time-dependent function of the radiative intensity penetrating on the front surface of the honeycomb component has been calculated as an upper limit of the thermal loads occurring during regular operation of a solar tower power plant. For convenience, the radiation has been assumed to be homogeneously distributed onto the absorber front surface. The function is shown in Figure 3. Since the absorber module front surface consists of a central part and a sloped region at the edges, a second

function has been assumed for this edge region, taking into account the higher incident angles of the reflected solar beams in this region.

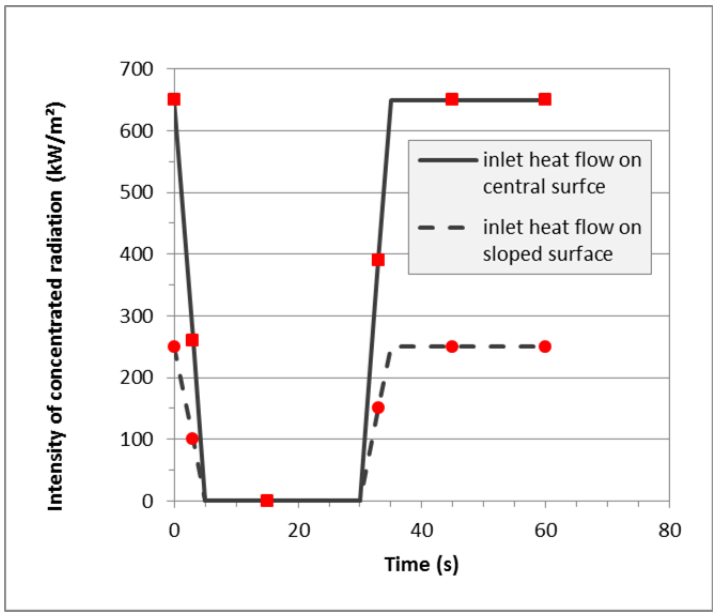

Figure 3**.** Time-dependent intensity of the solar flux as a consequence of the “cloud effect”

2.3 Coupled flow/heat transport model and thermo-mechanical model

The coupled flow/heat transport model has been developed by means of the commercial software COMSOL Multiphysics, whereas the thermo-mechanical model has been worked out with ANSYS. The honeycomb in-lay of the absorber module shown in Figure 4 has been considered as a representative solar absorber and calculated volume to be investigated. The cup made of dense SiSiC-ceramics has not been taken into account. Two different cell-densities have been analyzed. One can be denoted as the state-of-the-art technology, it has been approved in numerous experimental tests [16]. The other one has been manufactured for testing purposes. In prior studies, this geometry turned out to show a slightly higher solar-to-thermal efficiency [17]. A cross-sectional view of both geometries is shown in Figure 2. In the further course of the text, the two variants are called “standard” and “advanced geometry”.

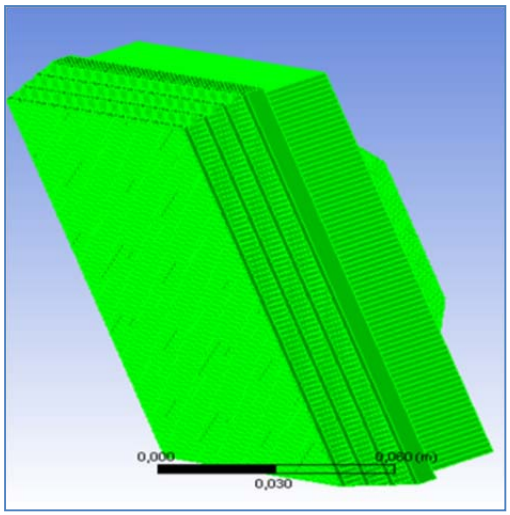

Figure 4: Honeycomb structure volume as treated in the model calculations

With the coupled flow/heat transfer model, the absorption of the concentrated solar radiation, which has been assumed to strike homogeneously onto the front surface of the component, the forced heat transfer to the air, which flows through the cells of the honeycomb structure and finally the free flow in each channel could be described. The latter has been treated with the weakly compressible Navier-Stokes equation according to a method already described in a prior article [16]. As main boundary conditions the solar radiation flux according to Figure 3 and the inlet air mass flow and temperature have been taken into consideration. The part of the solar radiation penetrating into the open channels has been regarded as an exponentially decreasing energy source term in the energy equation for the solid phase. The boundary conditions and material properties used are summarized in Table 1.

The temperature distribution from the combined flow/heat transfer model was imported into the ANSYS mechanical module as a boundary condition for the considered – real - honeycomb geometry of the absorber modules. Both geometry variants the advanced as well as the standard one have been imported. Due to the fineness of the structure, the grid had to fine as well resulting in long calculation times. Subsequently, the resulting stress distribution was obtained. Only compressive/tensile stresses (maximum stresses in the main coordinate axis) have been considered, shear stresses have not been taken into account, because it was likely that the observed cracks have been initiated as a consequence of tensile stresses.

Table 1. Boundary conditions and material properties used

Quantity and location	Boundary Condition
Inlet radiation flux central surface	0….650 kW/m²
Inlet radiation flux sloped surface	0…250 kW/m²
SiSiC specific heat capacity [18]	850 J/kg K
SiSiC thermal conductivity [18]	150...30 W/mK
Air inlet temperature	50°C
Air mass flow	0.013 kg/s

2.4 Determination of mechanical strength and real critical stresses

To determine the *mechanical strength* of the SiSiC honeycomb material, a conventional double-ring set-up was installed in a standard testing machine. Hereafter, 3 samples (size 50 x 50 x 10 $\pm$ 1 mm) of each kind, which have been cut out from the original absorber modules with a diamond saw, were loaded until fracture. The set-up – along with the equation for the standard evaluation method used for calculating the corresponding fracture stresses – is shown in Figure 5. The tests have been carried out according to an ISO-standard for metallic samples [19]. However, the stresses calculated according to this standard only describe the virtual maximum stresses of a corresponding imaginary dense sample. The real stresses in the struts of the cellular honeycomb are different. Thus, the fracture loads of the bending tests have been taken to load the *real* honeycomb in a numerical experimental using a mechanical model with ANSYS. The whole procedure including validation has been already published in a prior paper [20].

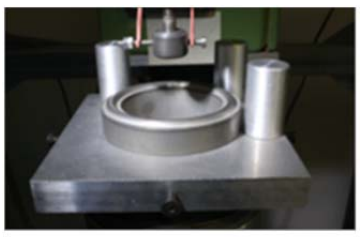

double ring bending test (1)

$$\sigma = 1.04 \cdot \frac{F_{max}}{h^2} \quad [\text{MPa}]$$

Figure 5**.** Double ring bending test set-up to determine the mechanical strength of the SiSiC honeycomb structure.

2.5 Experimental thermo-shock-tests

The experimental thermo-shock tests have been performed at the dish-test-bench which is in use on the Plataforma Solar de Almería (PSA) shown in Figure 6.

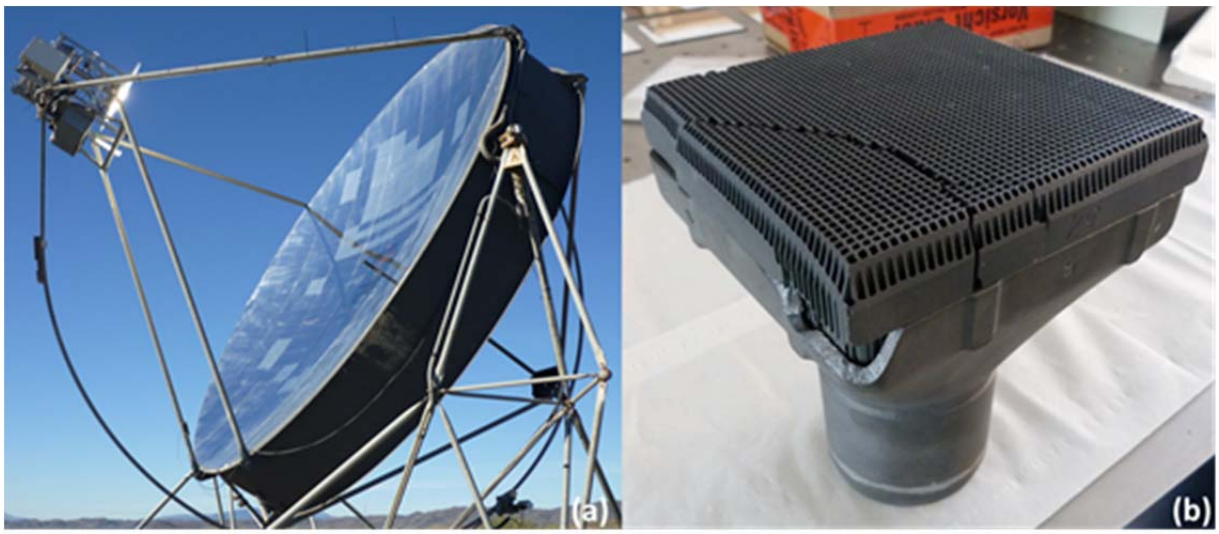

Figure 6. SiC volumetric absorber test bench in operation at DISTAL Dish-II concentrator on the Plataforma Solar de Almería (a) and cracked volumetric absorber cup (b)

The concept of this test bench is illustrated in Figure 7. The main air path consists of the open volumetric air absorber, a tube and a heat resistant air blower. The inbound ambient air is heated up in the absorber, flows through the inner tube and exits through the main blower into the environment. The absorber cup outlet temperature ($T_{\text{rec,out}}$) and mass flow ($\dot{M}_{air}$) are measured in the tube. It can be controlled by the rotation speed of the blower.

A second tube with bigger diameter covers the inner tube to simulate the return air of the volumetric receiver concept. The return air, which is - in this case - cold ambient air conveyed by a second blower, flows through the gap between the tubes in reverse direction and heats up by heat exchange with the hot inner tube. The return air temperature is measured just before it leaves through the gap between the absorber cup and the box, which encloses the cup. Also the air return temperature can be controlled by the blower speed. If no return air is needed, the mechanical slide valve in the annular gap can be closed and the slide valve on the surface of the outer tube opened, so the return air keeps cooling the inner tube.

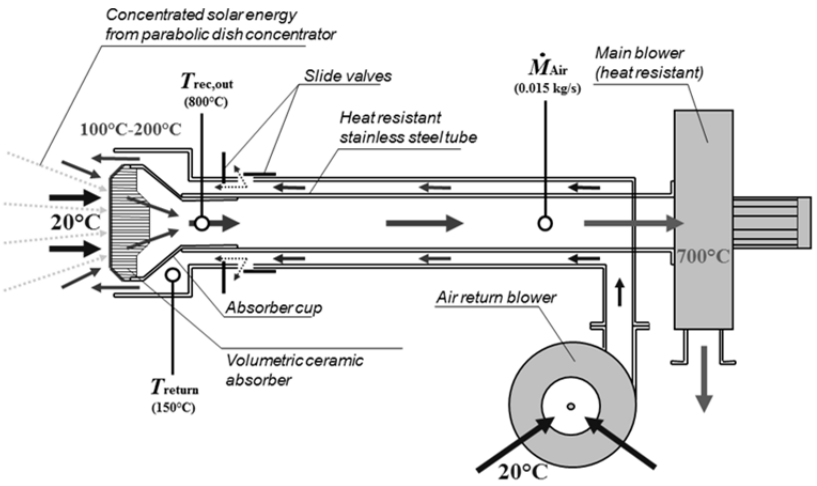

Figure 7. Flow chart of the volumetric absorber test bench at PSA

The following procedure is followed to test the thermo-shock resistance:

- The air mass flow flowing through the tested SiC honeycomb is 0.015 ± 0.005 kg/s
- The temperature of the air stream is directly measured behind the absorber cup with at least three thermocouples. The average value is considered
- The air stream is heated up to 750 ± 20°C. After reaching the maximum temperature, the air is cooled down to 200±20°C
- The sample is heated and cooled down for 15 times corresponding to a heating and cooling rate of the air of 250 ± 50 K/min
- A second air stream of 150 ± 50°C with no specified mass flow circulates around the absorber cup in opposite direction with respect to the main air flow to simulate the recirculation in power towers

The flux gradient on the front surface of the tested specimen is less than 40kW/m²/cm. This value is approximately 10 times higher than flux gradients appearing in a 1-MW solar power tower.

3. RESULTS AND DISCUSSION

3.1 Calculated time dependent temperature distributions

By means of the coupled flow/heat transfer problem described in the last section, the transient temperature distribution inside the two investigated absorber modules as a consequence of the cloud transition has been determined. The result is shown in Figure 8. The first row belongs to the standard geometry and the second row to the module with advanced geometry. The left image in each row represents the stationary case for full (lay-

out) radiative load of 650 kW/m². The next two ones represent the cases after 3 and 15 seconds after the onset of decrease of radiation as a consequence of the “cloud effect” and the next three ones represent the cases after 3, 15 and 30 seconds after the re-increase of the radiative power. The time-points are additionally illustrated as red dots in the load curve in Figure 3. It can be seen that as a consequence of the cloud transition the front surface cools down from the from 1234°C to 864°C in the case of the standard geometry and from 1043°C to 749°C in case of the advanced geometry.

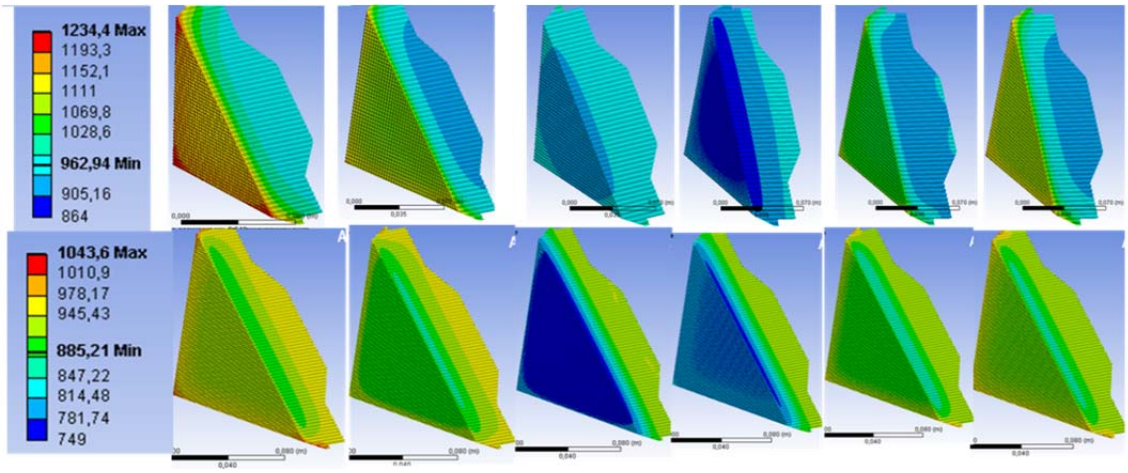

Figure 8. Temperature distribution at various times during the “cloud transition”. Upper row: standard geometry; lower row: advanced geometry. The exact time points are visualized in Figure 3 as red dots.

The corresponding air outlet temperature is shown in Figure 9 along with the cooling rates, which are assumed to be a measure for the intensity of the thermal load. These have been calculated additional to the solid temperature of the absorber, which is responsible for the stresses, to enable a comparison with the air outlet-temperatures and heating rates measured in the experimental themo-shock tests. It can be seen, that the air temperature responds to the “cloud transition” with a time delay of app. 40-50 seconds. The maximum cooling rate appears with a delay of about 36 seconds and is much higher in case of the advanced structure, which is quite clear since the overall heat transfer surface for solid-to-gaseous heat transfer is much larger in this case.

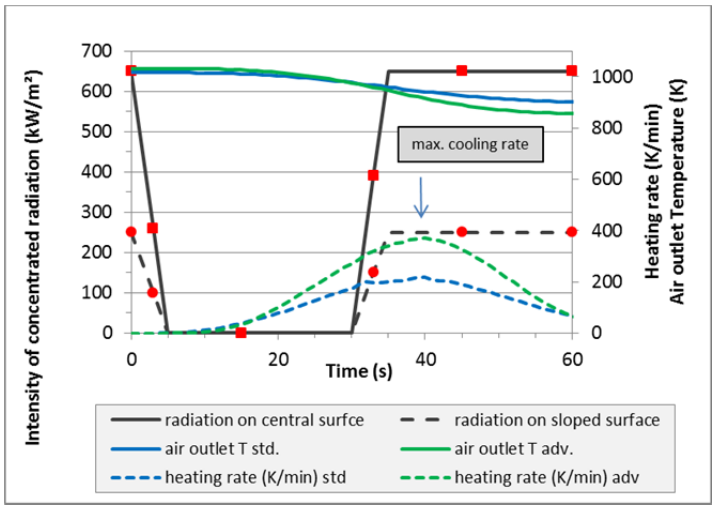

Figure 9. Outlet air temperatures and cooling rates calculated with the coupled flow/heat transport model

3.2 Determination of the corresponding stresses

Stress calculations have been carried out for a number of temperature distributions such as those shown in Figure 8. It turned out that the maximum stresses in both modules occurred approx. 30 seconds after the start of the "cloud transition". The stress distributions at that time are shown in Figure 10.

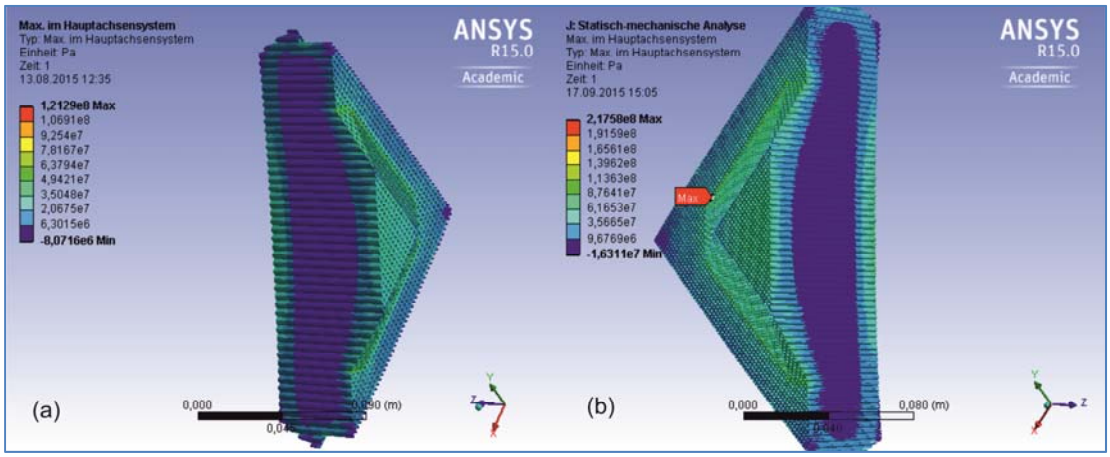

Figure 10. Stress distribution 30 seconds after start of the "cloud transition" in the standard structure (a) and the advanced structure (b)

A further comparison of the two investigated variants shows that the maximum stress in the advanced structure (approx. 218 MPa) is much larger than the one in the standard structure (121 MPa).

Secondly, it can be observed, that the maximum stress occurs app. 6 seconds before the maximum temporal thermal gradiant of the air outlet temperature. The complete maximum stress vs. time curve is shown in Figure 13.

3.3 Determination of the bending strength and critical stresses of the material

As described in section 2.5 the maximum bearable stresses in the cellular structure of the SiSiC honeycomb have been determined with a combination of conventional experimental bending tests and additional FEM-calculations. This procedure has become necessary since the fracture stresses delivered by a conventional bending tests treat the sample as a homogenuous, dense sample. It doesn't take into account the honeycomb structure in which the "real stresses" are much higher. The "effective" fracture stress values from the test and additionally the corresponding calculated real stresses is information allow us to estimate whether the thermal loads are below or above critical values. Furthermore, it should indicate whether the advanced structure is less or more resistant to thermal loads. Figure 11 illustrates the stress distribution in the two investigated variants during the bending test at fracture load. Table 2 summarizes the acquired results. As expected, the strength of the conventional honeycomb – calculated with the Iso-Standard - is much larger than the advanced one (22 MPa vs. 14 Mpa). This is of course low when compared with dense SiC ceramics. However, the maximum real stress at fracture load turns out to be 108 MPa in the conventional and 174 MPa in the advanced structure. This shows that the outer load is much more homogeneously distributed in the conventional structure, whereas the advanced geometry tends to have stress peaks in its thin walls.

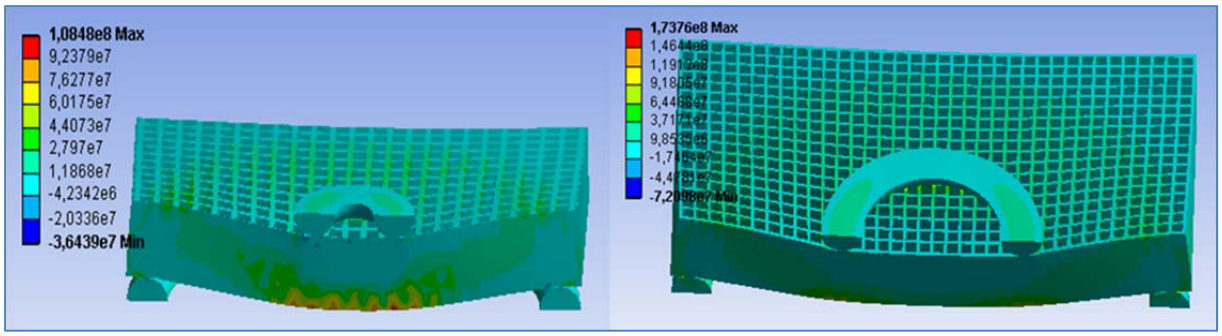

Figure 11. Calculated stress in the principal coordinate system during the double ring bending test (at fracture load) for the 80cpsi (left) and for the 200cpsi samples (right)

Table 2. Comparison of the fracture parameters of the investigated structures

absorber type	specimen thickness h [mm]	fracture load F_{max} [N]	fracture stress as calculated from iso-standard (MPa)	real fracture stress [MPa]
standard (80 cpsi)	9.36	1839	22	108
advanced (200 cpsi)	8.67	1026	14	174

3.4 Results of the experimental thermo-shock tests

The experimental thermo-shock test did not show the expected results. 3 of each type of absorbers have been exposed to thermal loads of different levels. As “thermal load” the heating/cooling rate of the air outlet temperature of the absorber sample is denoted. This has become a usual practice when operating a solar volumetric air receiver. For each sample at start, the average thermal load was set to approx. 200 K/min. After that, the load has been incrementally increased. However, due to influence from the ambient, mainly wind, this as controlled average thermal load may be markedly violated with the consequence that “short-term” thermal loads occur, which are up to 2 times higher.

In Figure 12, the data of one thermal shock experiment is shown as an example. Air outlet temperature and heat load appear as the blue and red curve respectively. After having received a thermal load of more than 300 K/min for app. 40 seconds, the absorber broke. The noise emitted when the absorber cracked was recorded using a microphone, allowing to determine the point in time when the failure occurred. This technique only worked for the sample shown in Figure 12 as wind or other noise sources disturbed the microphone signal. The entire results are comprised in Table 3. It can be seen that for the 200 cpsi materials a thermal load of 200 K/min was no problem. Going to larger loads two of the three samples broke, only one has withstood larger loads of up to 400 K/min. The three 80 cpsi cups show a contradictory view. Whereas one sample also withstood hard loads of more than 500 K/min and short term load of more than 1200 K/min (!) two others already broke at 200 K/min. From this only the very rough conclusion may be extracted that thermal loads of 200 K/min or more might be critical for both types of material. The location of the crack initiation has

not been investigated in detail. From the crack path it seemed likely that at the corners of the channels stress concentrations (notch effect) on the one hand facilitate the initiation of cracks and on the other hand also lead to crack propagation in the diagonal direction.

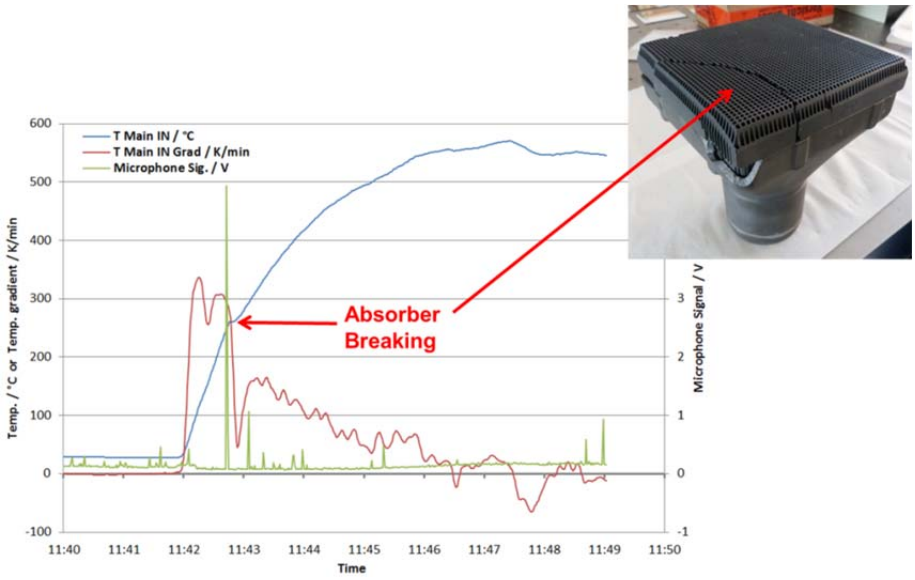

Figure 12: Example of an experimental thermo-shock test

Table 3: Results of the experimental thermo-shock tests

sample ID	**cell density** (cpsi)	**av. thermal load** (K/min)	**peak thermal load** (K/min)	**no. of cycles**	**failure** 1=yes 0=no
48	200	200-350	703	31	1
61	200	200-350	354	34	0
63	200	200-400	470	49	1
c1	80	200-500	1283	66	0
c2	80	200	253	13	1
c3	80	200	288	10	1

3.5 Comparison of model predictions and tests

Finally, the acquired numerical data has been compared with the experimental one. Clearly, the basic population - that is the number of experiments in the thermo-shock tests - was too low. Therefore they cannot serve as a validation of the numerical model. However, a rough comparison may be taken in a sense that a thermal load of heating/cooling rates of the air exit temperature in the range of 200 K/min or more must be seen as critical for the material. So far the experiments at least do not contradict the numerical results. In Figure 13, the experimental and numerical results are summarized. The maximum load inside the two material variants is represented as a function of time and these curves are compared to the

fracture stresses from the bending tests (bold dashed lines). It can be seen, that for both materials the calculated mechanical stress due to the heat load exceeds the critical (allowed) loads from the fracture tests markedly. Additionally, the estimated critical values from the thermos-shock experiments appear as thin dashed lines in the diagram. To achieve these latter values, the maximum of the numerically calculated stress curves in Figure 13 have been assigned to the max. thermal loads from Figure 9 and a linear realationship between those quantities has been assumed. With this linear relationship, the estimated rough critical experimental threshold of app. 200 K/min could be converted into stress values. These have been calculated to 120 MPa for the standard material and 144 MPa for the advanced one.

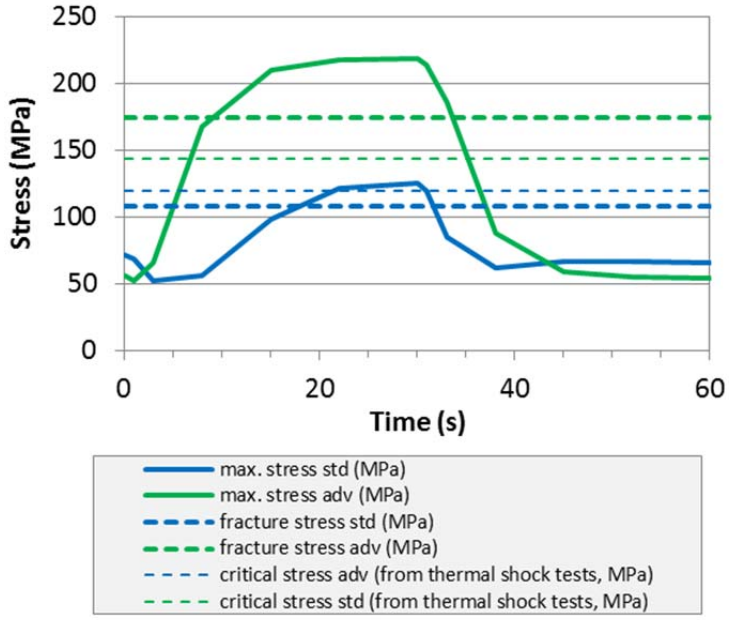

Figure 13: Comparison of the calculated with experimental data

4 CONCLUSIONS

The main conclusion to be drawn is that during regular operation of the absorber no critical thermal stresses occur. This also includes start-up and shut-down procedures as well as cloudy weather conditions. Furthermore it can be concluded that thermal stresses above app. 100 MPa in case of the standard material and 170 MPa in case of the advanced material should be avoided. This corresponds to heating rates of 100 and 150 K/min respectively. The thermal load case studied, in which extreme weather conditions have been assumed, led to significantly higher stresses. This means in practice, that in such a case the thermal load

shoud be minimized by operational means, for example a partial defocus in an appropriate time before the cloud transition.

The study has also shown an unacceptably large scatter of the experimental themo-shock results. This shows that the heating and cooling rate of the air outlet temperature is not an appropriate measure for the real thermal load of the employed material. A direct measurement of the material temperature (e.g by thermographical methods) should deliver more reliable results and the heating rate of the solid temperature should be of a clearer influence on to the stress conditions inside the absorber material.

ACKNOWLEGEMENTS

The work has been funded by the German Federal Ministry of Economic Affairs and Energy. The support is greatfully acknowleged.

REFERENCES:

[1] Fr. Aldinger, Werkstoffe, die die Welt verändern, Physikalische Blätter 55 (1999) 11.

[2] H. Fricker, Studie über die Möglichkeiten eines Alpenkraftwerkes, Bull. SEV/VSE, 76 (1997) 10-16.

[3] M. Romero, R. Buck, J. E. Pacheco, An Update on Solar Central Receiver Systems, Projects, and Technologies, Journal of Solar Energy Engineering 124 (2002) 98-108.

[4] A. Kribus, R. Zaibel, D. Carrey, A. Segal, J. Karni, A solar – driven combined cycle power plant, Solar Energy 62, 2 (1998) 121–129.

[5] Th. Fend, B. Hoffschmidt, R. Pitz–Paal, O. Reutter, Cellular ceramics use in solar radiation conversion, in: M. Scheffler and P. Colombo (eds.), Cellular ceramics: structure, manufacturing and applications, Willey – VCH GmbH & Co. KgA, Weinheim, 2005, pp. 523 – 546.

[6] Th. Fend, B. Hoffschmidt, R. Pitz–Paal, O. Reutter, P. Rietbrock, Porous materials as open volumetric solar receivers experimental determination of thermophysical and heat transfer properties, Energy 29, 5-6 (2004) 823 – 833.

[7] C. Agrafiotis, I. Mavroidis, A. Konstandopoulos, B. Hoffschmidt, P. Stobbe, M. Romero, V. Fernandez-Quero, Evaluation of porous silicon carbide monolithic honeycombs as volumetric receivers/collectors of concentrated solar radiation, Solar Energy Materials & Solar Cells 91 (2007) 474 – 488.

[8] A.L. Avila-Marin, Volumetric receivers in Solar Thermal Power Plants with Central Receiver System technology: A review, Solar Energy 85, 5 (2011) 891-91.
[9] B. Hoffschmidt, F. Tellez, A. Valverde, J. Fernandez, V. Fernandez, Performance Evaluation of the 200-kWth HiTRec-II Open Volumetric Air Receiver, Transactions of the ASME 94, 125 (2003).
[10] R. Capuano, Th. Fend, P. Schwarzbözl, O. Smirnova, H. Stadler, B. Hoffschmidt, R. Pitz-Paal, *Numerical models of advanced ceramic absorbers for volumetric receivers*, Renewable & Sustainable Energy Reviews, 58 (2016) 656–665.
[11] A. Kribus, H. Ries, W. Spirkl, Inherent limitations of volumetric solar receivers, Journal of Solar Energy Engineering 118 (1996) 151–155.
[12] Z. Wu, C. Caliot, G. Flamant, Z. Wang, Numerical simulation of convective heat transfer between air flow and ceramic foams to optimise volumetric solar air receiver performances, International Journal of Heat and Mass Transfer 54 (2011) 1527–1537.
[13] Wu, Z., Wang, Z., 2013, Fully coupled transient modeling of ceramic foam volumetric solar air receiver, Solar Energy 89 (2013) 122–133.
[14] R. Capuano, Th. Fend, B. Hoffschmidt, R. Pitz-Paal, Innovative VOLUMETRIC Solar Receiver Micro-design based on Numerical Predictions, 15th International Mechanical Engineering Congress & Exposition, IMECE 15, Houston, TX, USA (2015)
[15] M. Becker, Th. Fend, B. Hoffschmidt, R. Pitz–Paal, Theoretical and numerical investigation of flow stability in porous materials applied as volumetric solar receivers, Solar Energy 80 (2006) 1241 – 1248.
[16] Th. Fend, P. Schwarzboezl, O. Smirnova, D. Schöllgen and Ch. Jakob, Numerical Investigation of Flow and Heat Transfer in a Volumetric Solar Receiver, Renewable Energy 60 (2013) 655-661.
[17] Th. Fend, High porosity materials as volumetric receivers for solar energetics, Optica Applicata, Vol. XL, (2010).
[18] R.G. Munro, Material Properties of a Sintered α-SIC, J.Phys. Chem. Ref. Data 26, 5 (1997)
[19] Metallic materials - Bend test (ISO 7438:2005), German version EN ISO 7438:2005
[20] Th. Fend, P. Schwarzboezl, O. Smirnova, M. Schmücker, F. Flucht and S. Dathe, Thermo-mechanical Analysis of a Silicon Carbide Honeycomb Component applied as an absorber for concentrated solar radiation, 11th CMCME, Vancouver, June 14-19 (2015)